PHYSICAL REVIEW D **89,** 043528 (2014)

Application of the beyond δN formalism: Varying sound speed

Yu-ichi Takamizu*

Yukawa Institute for Theoretical Physics, Kyoto University, Kyoto 606-8502, Japan and
Department of Applied Mathematics and Theoretical Physics,
University of Cambridge, Wilberforce Road, Cambridge CB3 0WA, United Kingdom

(Received 6 December 2013; published 28 February 2014)

We focus on the evolution of curvature perturbation on superhorizon scales by adopting the spatial gradient expansion and show that the nonlinear theory, called the beyond δN formalism as the next-leading order in the expansion. As one application of our formalism for a single scalar field, we investigate the case of varying sound speed. In our formalism, we can deal with the time evolution in contrast to δN formalism, where curvature perturbations remain just constant, and nonlinear curvature perturbation follows the simple master equation whose form is similar to one in linear theory. So the calculation of bispectrum can be done in the next-leading order in the expansion as similar as the case of deriving the power spectrum. We discuss localized features of both primordial power and bispectrum generated by the effect of varying sound speed with a finite duration time. We can see a local feature like a bump in the equilateral bispectrum.

DOI: 10.1103/PhysRevD.89.043528 PACS numbers: 98.80.-k, 98.80.Cq

I. INTRODUCTION

Recent observations of the cosmic microwave background anisotropy, such as WMAP and PLANCK satellites [1,2], show very good agreement of the observational data with the prediction of standard inflationary cosmology where primordial fluctuations generated from quantum fluctuations of an inflaton field (see [3] for review). The most recent observations by the PLANCK [4,5] show that the primordial curvature perturbation is nearly scale invariant and follows almost perfect Gaussian statistics. The non-Gaussianity of primordial fluctuations is a powerful probe to discriminate inflationary models and also distinguish among different models (see, e.g., Ref. [6] and references therein). Therefore, if any tiny signature from these observations will be detected, it can tell us important information on the physics behind inflation. The PLANCK data [5] have measured $-8.9 < f_{\rm NL}^{\rm loc} < 14.3$ and $-192 < f_{\rm NL}^{\rm eq} < 108$ for the so-called local type and equilateral type of non-Gaussianity, respectively, at the 2σ (95%) confidence level. These observations show that the primordial curvature perturbation follows almost perfect Gaussian statistics, however it may be detected at smaller scales and also as some tiny localized feature in the bispectrum. Especially, although the quantity $f_{\rm NL}^{\rm loc}$ is now constrained very strongly, the possibility still remains that non-Gaussianity of equilateral shape has localized features. If ever detected, it would tell us important properties of the curvature perturbation and be a probe to distinguish the models of inflation.

The gradient expansion approach [7–19] to discuss the evolution of nonlinear curvature perturbation on superhorizon scales is a powerful tool on calculation as well as the second-order perturbation theory [20,21]. The lowest order in the expansion is the so-called δN formalism [9,12]. However, if we would analyze local features of the equilateral bispectrum, this formula is not suitable since it leads to that nonlinearity of curvature perturbations on long-wavelength scales over horizon always generates the local shape of bispectrum. Therefore we focus on the nonlinear theory valid to the next-leading order in the expansion. It is called the beyond δN formalism and it is able to give us not only the local, but also the equilateral shape of bispectrum in contrast to δN formalism, even though the expansion technique is taken on superhorizon scales [16,18]. Our nonlinear theory of the next-leading order in the expansion includes such subhorizon effect corresponding to the equilateral shape by matching a superhorizon curvature perturbation and subhorizon one suitably.

The main purpose of this paper is to investigate the situation where effective sound speed changes with a finite duration time and analyze whether features can appear in the bispectrum, in particular of the equilateral shape by using our nonlinear perturbation theory. The previous papers have studied the models of varying sound speed both in the power spectrum and in the bispectrum [22–29] (see also, e.g., [30–32] for the heavy physics, related to the same purpose and references therein), where one basically assumed a sudden change; however, we particularly focus on the effect of a finite duration time. As a simple application of beyond δN formalism, we will consider a single scalar field whose effective sound speed will change in time due to a noncanonical kinetic term. As a first step, we will assume the background evolution follows a simple slow-roll inflation, although a more realistic situation would be realized for a more complicated coupled kinetic term on a multiscalar system, such as the curvaton scenario [33,34], otherwise the slow-roll conditions will be also

*takamizu@yukawa.kyoto-u.ac.jp; yt313@cam.ac.uk

violated. However, in this paper in order to extract the effects of the change of sound speed alone, we study the case of varying sound speed without affecting the background evolution as a simple tractable example, the same setup as in Ref. [23], and see the Appendix therein for a more detailed discussion.

The rest of the paper is organized as follows. In Sec. II, we review beyond δN formalism and especially focus on the point that the master equations of curvature perturbation in linear and nonlinear theory show similar forms and derive the calculations. Then we discuss the possible example as the case of varying sound speed in Sec. III and derive featured power spectrums and bispectra of the curvature perturbations affected by such changes. Section IV is devoted to the conclusion.

II. BEYOND δN FORMALISM

We employ the spatial gradient expansion. In this approach, we suppose that the characteristic length scale L of a perturbation is longer than the Hubble length scale $1/H$ of the background, i.e. $\mathrm{HL} \gg 1$. Therefore, $\epsilon \equiv 1/(\mathrm{HL})$ is regarded as a small parameter and we can systematically expand equations in the order of ϵ, identifying a spatial derivative is of order ϵ, $\partial_i Q = \mathcal{O}(\epsilon)Q$. To clarify the order of gradient expansion, we introduce the superscript (m) to a quantity of order of gradient expansion: $\mathcal{O}(\epsilon^m)$.

The gradient expansion technique has been applied up to second order $\mathcal{O}(\epsilon^2)$ in the expansion to a universe dominated by a single [13–16] and a multiscalar field [18], yielding the formalism "beyond δN." The formulas have been also extended to be capable of a universe filled with a most generic noncanonical scalar field [19], which can give the so-called G-inflation. In this paper, we will consider a single scalar field as a simple example, whose kinetic term is a noncanonical, whose Lagrangian takes the form $P(X,\phi)$, where $X = -\partial^\mu\phi\partial_\mu\phi/2$ because we will later discuss the situation of the effective sound speed: $c_s^2 = P_X/(P_X + 2P_{XX}X)$ changes in time where the subscript X represents a derivative with respect to X and notice that the Lagrangian denoted by P plays the role of the pressure as shown in Refs. [15,35].

Following Ref. [16], we will briefly review beyond δN formalism for a single scalar field in this section. This system is characterized by a single scalar degree of freedom, and hence one expects that a single master variable governs the evolution of scalar perturbations even at nonlinear order. By virtue of gradient expansion, one can indeed derive a simple evolution equation[1] for an appropriately defined master variable $\mathcal{R}_c^{\mathrm{NL}}$ on comoving hypersurfaces:

$$\mathcal{R}_c^{\mathrm{NL}\prime\prime} + 2\frac{z'}{z}\mathcal{R}_c^{\mathrm{NL}\prime} + \frac{c_s^2}{4}R^{(2)}[\mathcal{R}_c^{\mathrm{NL}}] = \mathcal{O}(\epsilon^4), \quad (2.1)$$

with

$$z \equiv \frac{a}{H}\left(\frac{\rho+P}{c_s^2}\right)^{\frac{1}{2}}, \quad (2.2)$$

where ρ and P denote energy density and pressure of a scalar field, respectively, the prime represents differentiation with respect to the conformal time τ and $R^{(2)}[X]$ is the Ricci scalar of the metric X, which can be given by

$$R^{(2)}[\ell^{(0)}] = -2(2\Delta\ell^{(0)} + \delta^{ij}\partial_i\ell^{(0)}\partial_j\ell^{(0)})e^{-2\ell^{(0)}}. \quad (2.3)$$

We have taken the metric of the background spacetime as the flat FLRW universe,

$$ds^2 = a^2(-\alpha^2 d\tau^2 + e^{2\ell}\delta_{ij}dx^i dx^j) + \mathcal{O}(\epsilon^3), \quad (2.4)$$

where α denotes the lapse function, while the shift vector β^i is vanishing at the next-leading order $\beta^i = \mathcal{O}(\epsilon^3)$. As shown in [16,18], the natural assumptions on the metric is $\beta^i = \mathcal{O}(\epsilon)$ since the FLRW background must be recovered in the limit $\epsilon \to 0$. However, we assume the absence of any spatial gradient at leading order and the universe is locally homogeneous and isotropic. This leads to the above stronger condition and can be justified by the choice of the spatial coordinates.

Equation (2.1) is to be compared with its linear counterpart:

$$\mathcal{R}_c^{\mathrm{Lin}\prime\prime} + 2\frac{z'}{z}\mathcal{R}_c^{\mathrm{Lin}\prime} - c_s^2\Delta\mathcal{R}_c^{\mathrm{Lin}} = 0, \quad (2.5)$$

from which one notices the correspondence between the linear and nonlinear evolution equations. In order to calculate the evolution equations in Fourier space, we have to take the replacement $\Delta \to -k^2$.

It is important to notice that the structures of both (2.1) and (2.5) are similar forms, except for the last terms in the left-hand sides. This point is an advantage in order to estimate evolutions of curvature perturbations in linear and nonlinear theory since the same calculation is valid on following the evolution equation. We will see the details later.

A. Linear theory valid through $\mathcal{O}(\epsilon^2)$

To obtain the power spectrum, we will use the linear theory of the curvature perturbation in this subsection. The above equation (2.5) has two independent solutions; conventionally called a growing mode and a decaying mode.

[1] Also for a generic noncanonical single scalar field, the master equation becomes a simple evolution equation as a same form. As shown in Ref. [19], the system described by the so-called G-inflation, that is $P(X,\phi) - G(X,\phi)\Box\phi$ can be reduced to a same form with an extended definition of z.

We assume that the growing mode is constant in time at leading order in the spatial gradient expansion.

As shown in [16], the linear solution valid up to $\mathcal{O}(\epsilon^2)$ can be obtained as

$$\mathcal{R}^{\rm Lin}_{c,\boldsymbol{k}}(\tau) = \left[\tilde{\alpha}^{\rm Lin}_{\boldsymbol{k}} + (1-\tilde{\alpha}^{\rm Lin}_{\boldsymbol{k}})\frac{\tilde{D}(\tau)}{\tilde{D}_*} - \left(\frac{\tilde{F}_*}{\tilde{D}_*}\tilde{D}(\tau)+\tilde{F}(\tau)\right)k^2\right]U^{(0)}_{\boldsymbol{k}}, \quad (2.6)$$

where the integrals $\tilde{D}(\tau)$ and $\tilde{F}(\tau)$ have been given as

$$\tilde{D}(\tau) = 3\mathcal{H}(\tau_*)\int_{\tau_*}^{\eta} d\tau' \frac{z^2(\tau_*)}{z^2(\tau')},$$
$$\tilde{F}(\tau) = \int_{\tau_*}^{\tau}\frac{d\tau'}{z^2(\tau')}\int_{\tau_*}^{\tau'} z^2(\tau'')c_s^2(\tau'')d\tau''. \quad (2.7)$$

Here $\tilde{D}_* = \tilde{D}(\tau_*)$, $\tilde{F}_* = \tilde{F}(\tau_*)$, τ_* and $\mathcal{H}$ denote an initial time of gradient expansion and the conformal Hubble parameter $\mathcal{H} = d\ln a/d\tau$, respectively. The integrals in (2.7) represent a decaying and growing mode solution, respectively.

Note that $\mathcal{R}^{\rm Lin}_{c,\boldsymbol{k}}(\tau_*) = U^{(0)}_{\boldsymbol{k}}$ that is just a constant solution, while $\mathcal{R}^{\rm Lin}_{c,\boldsymbol{k}}(0) = \tilde{\alpha}^{\rm Lin}_{\boldsymbol{k}}U^{(0)}_{\boldsymbol{k}}$. Thus if the factor $|\tilde{\alpha}^{\rm Lin}_{\boldsymbol{k}}|$ is large, it represents an enhancement of the curvature perturbation on superhorizon scales due the $\mathcal{O}(\epsilon^2)$ effect.

Here it is useful to consider an explicit expression for $\tilde{\alpha}^{\rm Lin}_{\boldsymbol{k}}$ in terms of $\mathcal{R}^{\rm Lin}_{c,\boldsymbol{k}}$ and its derivative at $\tau=\tau_*$. The result is

$$\tilde{\alpha}^{\rm Lin}_{\boldsymbol{k}} = 1 + \frac{\tilde{D}_*}{3\mathcal{H}_*}\frac{\mathcal{R}^{\rm Lin\prime}_{c,\boldsymbol{k}}(\tau_*)}{\mathcal{R}^{\rm Lin}_{c,\boldsymbol{k}}(\tau_*)} - k^2\tilde{F}_* + \mathcal{O}(k^4). \quad (2.8)$$

In order to relate our calculation with the standard formula for the curvature perturbation in linear theory, we introduce τ_k (or t_k) which denotes the time at which the comoving wave number has crossed the Hubble horizon,

$$\tau_k = -\frac{r}{k}; \qquad 0 < r \ll 1. \quad (2.9)$$

The power spectrum at the horizon crossing time is given by

$$\langle \mathcal{R}^{\rm Lin}_{c,\boldsymbol{k}}(\tau_k)\mathcal{R}^{\rm Lin}_{c,\boldsymbol{k}'}(\tau_{k'})\rangle = (2\pi)^3 P_{\mathcal{R}}(k)\delta^3(\boldsymbol{k}+\boldsymbol{k}'),$$
$$P_{\mathcal{R}}(k) = |\mathcal{R}^{\rm Lin}_{c,\boldsymbol{k}}(\tau_k)|^2. \quad (2.10)$$

By inverting $\mathcal{R}^{\rm Lin}_{c,\boldsymbol{k}}$ in terms of $U^{(0)}_{\boldsymbol{k}}$ as shown in [16], we can show the final value of the linear curvature perturbation as

$$\mathcal{R}^{\rm Lin}_{c,\boldsymbol{k}}(0) = \tilde{\alpha}^{\rm Lin}_{\boldsymbol{k}}U^{(0)}_{\boldsymbol{k}} = \alpha^{\rm Lin}_{\boldsymbol{k}}\mathcal{R}^{\rm Lin}_{c,\boldsymbol{k}}(\tau_k) + \mathcal{O}(k^4), \quad (2.11)$$

where

$$\alpha^{\rm Lin}_{\boldsymbol{k}} = 1 + \alpha^{\mathcal{R}}D_k - k^2F_k, \quad (2.12)$$

and

$$\alpha^{\mathcal{R}} = \frac{1}{3\mathcal{H}(\eta_k)}\left.\frac{\mathcal{R}^{\rm Lin\prime}_{c,\boldsymbol{k}}}{\mathcal{R}^{\rm Lin}_{c,\boldsymbol{k}}}\right|_{\tau=\tau_k},$$
$$D_k = 3\mathcal{H}(\tau_k)\int_{\tau_k}^{0} d\tau' \frac{z^2(\tau_k)}{z^2(\tau')},$$
$$F_k = \int_{\tau_k}^{0}\frac{d\tau'}{z^2(\tau')}\int_{\tau_k}^{\tau'} z^2(\tau'')c_s^2(\tau'')d\tau''. \quad (2.13)$$

The formula (2.11) will be used in the next subsection.

The power spectrum at the final time is thus enhanced by the factor $|\alpha^{\rm Lin}_{\boldsymbol{k}}|^2$ as

$$\langle \mathcal{R}^{\rm Lin}_{c,\boldsymbol{k}}(0)\mathcal{R}^{\rm Lin}_{c,\boldsymbol{k}'}(0)\rangle = (2\pi)^3|\alpha^{\rm Lin}_{\boldsymbol{k}}|^2 P_{\mathcal{R}}(k)\delta^3(\boldsymbol{k}+\boldsymbol{k}'). \quad (2.14)$$

B. Nonlinear theory valid through $\mathcal{O}(\epsilon^2)$

Using the linear solution of the curvature perturbation given by (2.6), here we can derive the nonlinear solution by matching the two at $\tau=\tau_*$. The main purpose of the matching is to make it possible to analyze superhorizon nonlinear evolution valid up to the second order in gradient expansion, starting from a solution in the linear theory. In particular, we would like to evaluate the bispectrum induced by the superhorizon nonlinear evolution. For this purpose, we need to have full control over terms up not only to $\mathcal{O}(\epsilon^2)$ but also to $\mathcal{O}(\delta^2)$. We have introduced a small expansion parameter δ that characterizes the amplitude of perturbation, where we suppose that the linear solution is of order $\mathcal{O}(\delta)$.

Therefore, the matching condition at $\tau=\tau_*$ should be of the form

$$\mathcal{R}^{\rm NL}_c(\tau_*) = \mathcal{R}^{\rm Lin}_c(\tau_*) + s_1(\tau_*) + \mathcal{O}(\epsilon^4,\delta^3),$$
$$\mathcal{R}^{\rm NL\prime}_c(\tau_*) = \mathcal{R}^{\rm Lin\prime}_c(\tau_*) + s_2(\tau_*) + \mathcal{O}(\epsilon^4,\delta^3), \quad (2.15)$$

where $s_1(\tau_*) = \mathcal{O}(\delta^2)$ and $s_2(\tau_*) = \mathcal{O}(\delta^2)$ are functions of τ_* and spatial coordinates. While the linear solution $\mathcal{R}^{\rm Lin}_c(\tau)$ is considered as an input, i.e., initial condition, the additional terms, $s_1(\tau_*)$ and $s_2(\tau_*)$, are to be determined by the following condition. The terms of order $\mathcal{O}(\delta^2)$ in $\mathcal{R}^{\rm NL}_{c,\boldsymbol{k}}$ and $\mathcal{R}^{\rm NL\prime}_{c,\boldsymbol{k}}$ should vanish at the horizon crossing when $\tau=\tau_k$. Note that $\tau_k < \tau_*$. In other words, $s_1(\tau_*)$ and $s_2(\tau_*)$ represent the $\mathcal{O}(\delta^2)$ part of $\mathcal{R}^{\rm NL}_c$ and $\mathcal{R}^{\rm NL\prime}_c$, respectively, generated during the period between the horizon crossing time and the matching time.

We have to omit the explicit way to determine the terms s_1 and s_2 for want of space, that was determined automatically and shown in [16]. Therefore, to match the solutions, we do not need to use the second order

perturbation theory and we have shown that the final result is independent from the the infinitesimal shift of the matching time; see [16].

As a result, using the linear solution of the curvature perturbation given by (2.6) we have the nonlinear comoving curvature perturbation at the final time $\tau = 0$ (or $t = \infty$) given by

$$\mathcal{R}^{\rm NL}_{c,\boldsymbol{k}}(0) = \mathcal{R}^{\rm Lin}_{c,\boldsymbol{k}}(\tau_k) - (1-\alpha^{\rm Lin}_{\boldsymbol{k}})\mathcal{R}^{\rm Lin}_{c,\boldsymbol{k}}(\tau_k) - \frac{1}{4}F_k\tilde{R}^{(2)}[\mathcal{R}^{\rm Lin}_{c}(\tau_k)] + \mathcal{O}(\epsilon^4,\delta^3), \tag{2.16}$$

where

$$\tilde{R}^{(2)}[\ell^0] \equiv -2(\delta^{ij}\partial_i\ell^0\partial_j\ell^0 - 4\ell^0\Delta\ell^0) = 4\Delta\ell^0 + R^{(2)}[\ell^0] + \mathcal{O}((\ell^0)^3). \tag{2.17}$$

The first term in (2.16) corresponds to the result of the δN formalism, which is a constant since we considered the system for a single scalar field, the second term is related to an enhancement on superhorizon scales in linear theory, and the last term is the nonlinear effect which may become important if F_k is large.

It is noticed that in order to calculate the final values of curvature perturbation both in linear (2.11) and in nonlinear theory (2.16), all one has to do is to estimate the same integrals shown in both theories as D_K and F_k in $\alpha^{\rm Lin}_{\boldsymbol{k}}$. The reason why is that the master equations (2.1) and (2.5) for both theories have the same structures of the evolution equation as described before.

In this subsection, we calculate the bispectrum of our nonlinear curvature perturbation by assuming that $\mathcal{R}^{\rm Lin}_{c,\boldsymbol{k}}(\tau_k)$ is a Gaussian random variable. We assume the leading order contribution to the bispectrum comes from the terms second order in $\mathcal{R}^{\rm Lin}_{c,\boldsymbol{k}}(\tau_k)$. The final result (2.16) can be reduced to

$$\zeta_{\boldsymbol{k}} = \mathcal{R}^{\rm NL}_{c,\boldsymbol{k}}(0) = \alpha^{\rm Lin}_{\boldsymbol{k}}\mathcal{R}^{\rm Lin}_{c,\boldsymbol{k}}(\tau_k) + \frac{F_k}{2}\left\{\int\frac{d^3k'd^3k''}{(2\pi)^3}(4k'^2 - \delta_{ij}k'^ik''^j) \times \mathcal{R}^{\rm Lin}_{c,\boldsymbol{k}'}(\tau_{k'})\mathcal{R}^{\rm Lin}_{c,\boldsymbol{k}''}(\tau_{k'})\delta^3(-\boldsymbol{k}+\boldsymbol{k}'+\boldsymbol{k}'')\right\} + \mathcal{O}(\epsilon^4,\delta^3). \tag{2.18}$$

By assuming the Gaussian statistics for $\mathcal{R}^{\rm Lin}_{c,\boldsymbol{k}}(\tau_k)$, it is easy to calculate the power spectrum shown as (2.14) with (2.10) and the bispectrum of primordial curvature perturbation: ζ.

The dimensionless bispectrum $\mathcal{B}_\zeta$ is expressed in terms of the Fourier transformation of the three point function as

$$\langle\zeta_{\boldsymbol{k}_1}\zeta_{\boldsymbol{k}_2}\zeta_{\boldsymbol{k}_3}\rangle_C = (2\pi)^7\delta^3(\mathbf{k}_1+\mathbf{k}_2+\mathbf{k}_3)\mathcal{P}^2_\zeta\frac{\mathcal{B}_\zeta}{k_1^2k_2^2k_3^2}, \tag{2.19}$$

where $\langle\cdots\rangle_C$ means that it extracts out only connected graphs. We use the dimensionless quantity $\mathcal{B}_\zeta$ to represent the amplitude of the bispectrum with the uncorrected power spectrum $\mathcal{P}_\zeta$, which has been defined by $\mathcal{P}_\zeta = k^3P_\zeta/2\pi^2$. We can use a standard amplitude of dimensionless power spectrum as $\mathcal{P}_\zeta = \mathcal{O}(10^{-9})$. With the help of ((2.18), the three point correlation function of ζ is at leading order calculated as

$$\langle\zeta_{\boldsymbol{k}_1}\zeta_{\boldsymbol{k}_2}\zeta_{\boldsymbol{k}_3}\rangle_C = (2\pi^3)[{\rm Re}(\alpha^{\rm Lin*}_{k_1}\alpha^{\rm Lin}_{k_2})F_{k_3} \times\{2(k_1^2+k_2^2) - \delta_{ij}k_1^ik_2^j\}\delta^{(3)}(\mathbf{k}_1+\mathbf{k}_2+\mathbf{k}_3) \times|\mathcal{R}^{\rm Lin}_{c,\boldsymbol{k}_1}(\tau_{k_1})|^2|\mathcal{R}^{\rm Lin}_{c,\boldsymbol{k}_2}(\tau_{k_2})|^2 + 2\,\text{terms}], \tag{2.20}$$

where Re means taking a real part, a superscript star denotes a complex conjugate and "2 terms" means terms with cyclic and permutations among the three wave numbers. The power spectrum of $\mathcal{R}^{\rm Lin}_{c,\boldsymbol{k}}(\tau_k)$ is written as (2.10). Then we have

$$\mathcal{B}_\zeta(k_1,k_2,k_3) = \frac{1}{8k_1k_2k_3}[{\rm Re}(\alpha^{\rm Lin*}_{k_1}\alpha^{\rm Lin}_{k_2})F_{k_3} \times\{5(k_1^2+k_2^2) - k_3^2\}k_3^3\Delta\mathcal{P}_\zeta(k_1)\Delta\mathcal{P}_\zeta(k_2) + 2\,\text{terms}], \tag{2.21}$$

where $\Delta\mathcal{P}_\zeta$ denotes the modulation factor of power spectrum, which is a ratio of a corrected power spectrum to an uncorrected one:

$$\Delta\mathcal{P}_\zeta(k) = \frac{k^3}{2\pi^2\mathcal{P}_\zeta}|\mathcal{R}^{\rm Lin}_{c,\boldsymbol{k}}(\tau_k)|^2. \tag{2.22}$$

III. APPLICATION: VARYING SOUND SPEED

We consider the case of varying sound speed as one application of beyond δN formalism. As a simple example, we have assumed that the background evolution satisfies the slow-roll conditions throughout this paper, that is

$$\eta_1 = -\frac{\dot{H}}{H^2} \ll 1 \quad\text{and}\quad \eta_2 = \frac{\dot{\eta}_1}{H\eta_1} \ll 1, \tag{3.1}$$

where a dot denotes a derivatives with respect to the physical time t. We compute the curvature perturbation for a model such that time variation of the sound speed is described by the following function as

$$c_s^2 = c_{s1}^2 + (c_{s2}^2 - c_{s1}^2)\frac{\tanh[(\tau-\tau_0)/d]+1}{2}, \tag{3.2}$$

where c_{s1}, c_{s2}, τ_0 and d are parameters and the sound speed changes from c_{s1} to c_{s2} with a varying duration characterized by τ_0 and d. We can introduce a new parameter

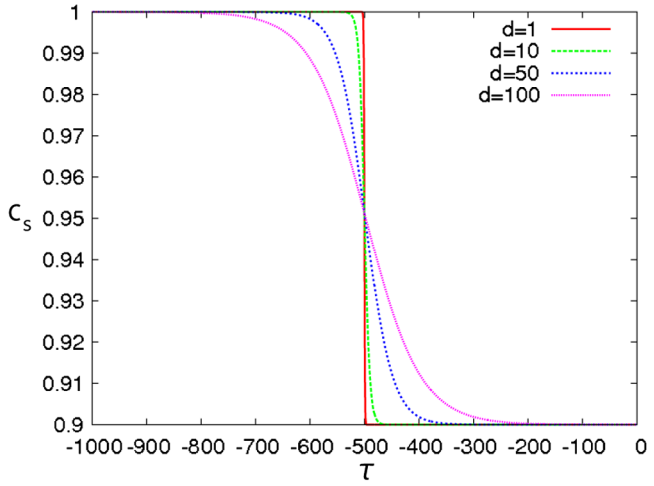

FIG. 1 (color online). We plot varying sound speed as taking $c_{s1} = 1$, $c_{s2} = 0.9$ for various values of varying width d. We set $\tau_0 = -500$. The horizontal axis is taking the conformal time.

$T = c_{s1}/c_{s2}$, which represents the ratio of sound speed before and after the transition. If we take the width of duration very small $d \lesssim 1$, the model results in the previous study of sudden varying sound speeds as in [23]. Throughout this paper, we set $\tau_0 = -500$, but the results do not depend on specifying the choice of the parameter. We plot the evolution of sound speed for example in Fig. 1 where we set $T = 0.9$ and $d = 1$, 10, 50, 100.

A. Power spectrum

The basic equation in the linear theory for primordial curvature perturbation ζ is written in terms of $v = \zeta z$. The basic equation of motion for Fourier modes is given by

$$v_k'' + \left(c_s^2 k^2 - \frac{z''}{z}\right) v_k = 0. \tag{3.3}$$

We introduce a variable u, which is related to v as

$$-c_s k^2 u_k = z\left(\frac{v_k}{z}\right)', \qquad c_s v_k = \theta\left(\frac{u_k}{\theta}\right)', \tag{3.4}$$

where we have defined $\theta \equiv 1/(c_s z)$. The basic equation of motion (3.3) in terms of the Fourier modes u_k is obtained as

$$u_k'' + \left(c_s^2 k^2 - \frac{\theta''}{\theta}\right) u_k = 0. \tag{3.5}$$

Note that the term (c_s'/c_s) does not exist in θ''/θ since the variable θ does not depend on c_s from (2.2) as $\theta = 1/(a\sqrt{2\eta_1})$. We have to solve this equation under the background evolution. The term θ''/θ is rewritten in terms of slow-roll parameters as

$$\frac{\theta''}{\theta} = \frac{1}{\tau^2}\left(\frac{\eta_2}{2} - \eta_1\right), \tag{3.6}$$

where we have used slow-roll approximation that is, $|\eta_1|$, $|\eta_2| \ll 1$ and taking their linear limits, and used a useful equation,

$$aH = -\frac{1}{\tau(1-\eta_1)}. \tag{3.7}$$

Therefore, we can obtain the basic equation

$$u_k'' + \left(c_s^2 k^2 - \frac{\nu^2 - \frac{1}{4}}{\tau^2}\right) u_k = 0, \tag{3.8}$$

where we have defined

$$\nu^2 = \frac{\eta_2}{2} - \eta_1 + \frac{1}{4}, \tag{3.9}$$

and approximate it as

$$\nu = \sqrt{\frac{\eta_2}{2} - \eta_1 + \frac{1}{4}} \approx \frac{1}{2} + \frac{\eta_2}{2} - \eta_1. \tag{3.10}$$

In the regime when $\tau < \tau_0$, setting $c_s = c_{s1}$ leads to the equation of motion,

$$u_k'' + \left(c_{s1}^2 k^2 - \frac{\nu^2 - \frac{1}{4}}{\tau^2}\right) u_k = 0, \tag{3.11}$$

and its solution is obtained by

$$u_{k1} = \sqrt{-kc_{s1}\tau}[c_1 H_\nu^{(1)}(-kc_{s1}\tau) + c_2 H_\nu^{(2)}(-kc_{s1}\tau)], \tag{3.12}$$

where $H_\nu^{(1),(2)}(\tau)$ denote the Hankel function and $c_{1,2}$ are arbitrary constants, which have to be determined by initial conditions at the time $\tau \to -\infty$. We choose the adiabatic vacuum at the initial time in terms of v_k as $v_k \to e^{-ikc_{s1}\tau}/\sqrt{2kc_{s1}}$. Hence it leads to the choice of c_1, c_2 as

$$c_1 = \frac{i}{2k^{3/2}}\sqrt{\frac{\pi}{c_{s1}}}\exp\left(\frac{2\nu+1}{4}\pi i\right), \qquad c_2 = 0. \tag{3.13}$$

We solve the basic equation (3.8) numerically with the above initial condition. This solution can show us the evolution from subhorizon scale to superhorizon scale. On the other hand, we can calculate the enhance factor $|\alpha_k^{\rm Lin}|$ by estimating the Eq. (2.13) obtained under the long-wavelength approximation. Then we can compare it with the above numerical exact solution. In order to compare them, we have to estimate ζ from the numerical solution of u by using the relation $\zeta = v/z = \theta^2(u/\theta)'$.

First we will show the exact solution by using numerical solving in the left panel of Fig. 2 for various values of d. We plot the modulation factors of power spectrum with k/k_0, where k_0 is the wave number corresponding to a transition time τ_0. It shows some feature like bump at $k = k_0$ with oscillation. As d takes a smaller value, the oscillations are more intensive and they do not converge for $d < \mathcal{O}(1)$. The

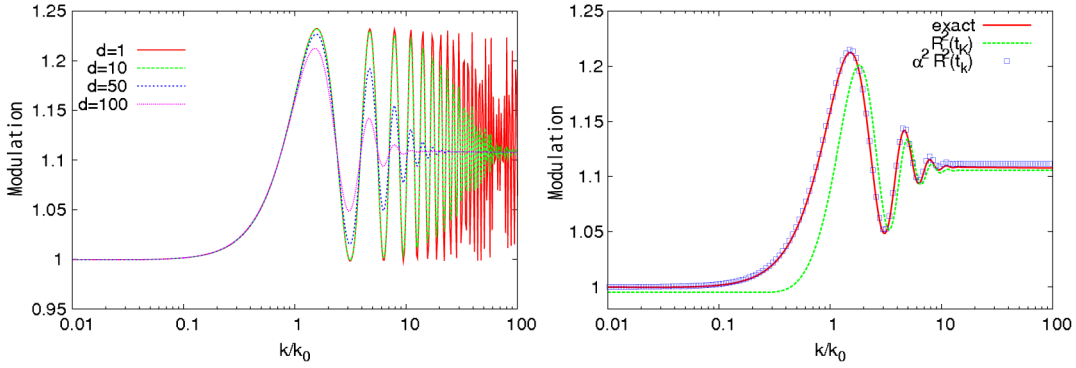

FIG. 2 (color online). (Left) We plot the modulation factor of final power spectrum for various values of d with setting $T = 0.9$. We can see the featured bumps at $k = k_0$ with oscillation. As d takes a smaller value, the oscillations are more intensive. (Right) Comparison the long-wavelength approximation (2.14) with the numerical exact solution of (3.8). We set $T = 0.9$ and $d = 100$. The enhancement from the amplitude at the horizon crossing time $\mathcal{R}^2(\tau_k)$ (green line), which is described by $(\alpha_k^{\mathrm{Lin}})^2$ of (2.12), occurs at superhorizon scales $k/k_0 < 1$.

result of $d = 1$ is consistent with the previous result of Ref. [23] for studying the case of a sudden varying sound speed.

The right panel of Fig. 2 shows the comparison of such an exact solution with the solution obtained by using the long-wavelength approximation as (2.14). It tells us that the approximation is very good for fitting the exact solution. Especially, we can see that the approximation is good for not only the superhorizon regime $k/k_0 < 1$, but also the subhorizon regime $k/k_0 > 1$. The enhancement from the amplitude at the horizon crossing time, which is described by $(\alpha_k^{\mathrm{Lin}})^2$ of (2.12), occurs at superhorizon scales $k/k_0 < 1$.

Next, we will examine how the modulation factors depend on different variables. In Fig. 3, we plot the final power spectrums for the case of decreasing sound speed $T < 1$ and

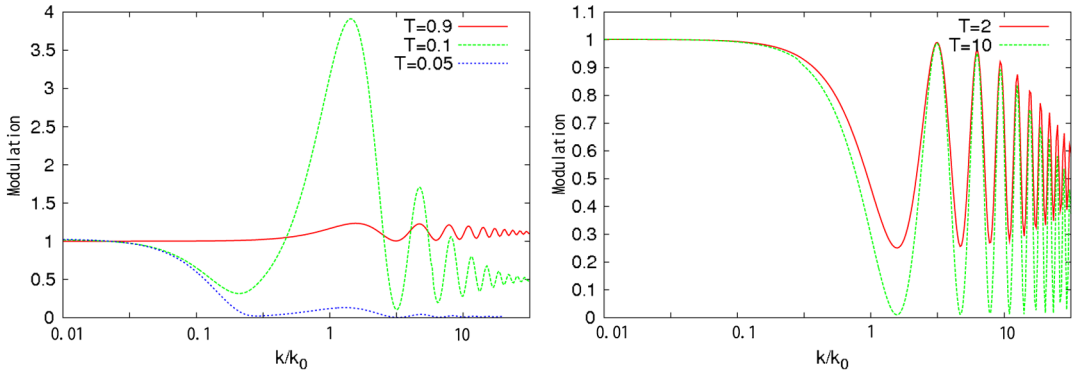

FIG. 3 (color online). We plot the modulation of final power spectrums for various values of $T < 1$ (left) and $T > 1$ (right) with setting $d = 20$. All cases in the left (right) panel correspond to the situations of decreasing (increasing) sound speeds.

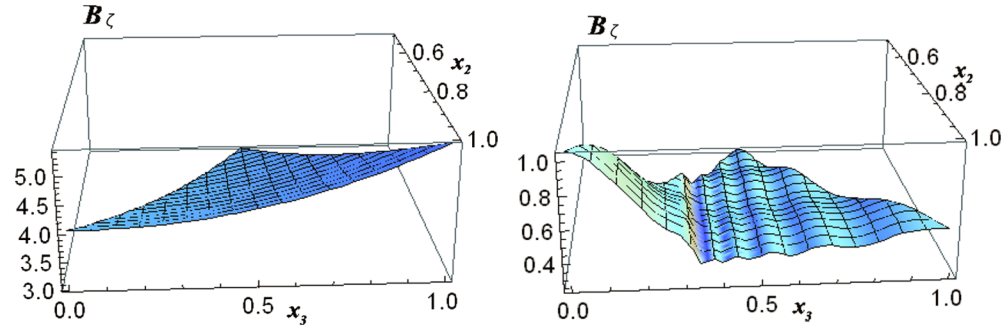

FIG. 4 (color online). We plot dimensionless bispectrum as a function of $x_2 = k_2/k_1$ and $x_3 = k_3/k_1$. We set $T = 0.5$, $d = 20$ with parameters: $k_1/k_0 = 0.1$ (left) and $k_1/k_0 = 1$ (right). The bispectrum has a peak at the equilateral (local) shape in the left (right) panel.

the increasing one $T > 1$, respectively. From the observation of WMAP, the parameter $|T-1| \gtrsim 0.1$ is strongly constrained, therefore the modulation appearing for $T = 0.9$ is at most in order to make features in power spectrum (see [23] for the details).

B. Bispectrum

In order to compare with observations, we can define a k-dependent nonlinear parameter by dividing the dimensionless bispectrum by a square of the corrected power spectrum at the final time: $f_{\rm NL}(k_1, k_2, k_3)$ as

$$f_{\rm NL} \equiv \frac{10}{3}\frac{k_1k_2k_3\mathcal{B}_\zeta}{|\alpha^{\rm Lin}_{\boldsymbol{k}_1}\alpha^{\rm Lin}_{\boldsymbol{k}_2}|^2\Delta\mathcal{P}_\zeta(k_1)\Delta\mathcal{P}_\zeta(k_2)k_3^3 + 2 \text{ terms}} = \frac{5}{12}\left[|\alpha^{\rm Lin}_{\boldsymbol{k}_1}\alpha^{\rm Lin}_{\boldsymbol{k}_2}|^2k_3^3 + 2 \text{ terms}\right]^{-1} \times \left[{\rm Re}(\alpha^*_{k_1}\alpha_{k_2})F_{k_3}\{5(k_1^2+k_2^2)-k_3^2\}k_3^3 + 2 \text{ terms}\right]. \tag{3.14}$$

Next we will plot k-dependent nonlinear parameter $f_{\rm NL}(k_1, k_2, k_3)$. We plot a dimensionless bispectrum as a function of $x_2 \equiv k_2/k_1$ and $x_3 \equiv k_3/k_1$ with the free parameter k_1/k_0 in Fig. 4. In the figure, we take $k_1/k_0 = 0.1$ and $k_1/k_0 = 1$, respectively for both of the same settings of $T = 0.5$, $d = 20$. Here we notice that our expansion technique is valid for $k_1/k_0 \leq 1$, since we can predict the evolution only when the transition happens after the horizon crossing, $t_k < t_0$. As shown in Fig. 4, for the small value of $k_1/k_0 < 1$, the bispectrum has a peak at an equilateral shape; $k_1 = k_2 = k_3$. On the other hand, for $k_1/k_0 = 1$, it has a peak at a local (squeezed) shape; $k_3 = 0$, $k_1 = k_2$.

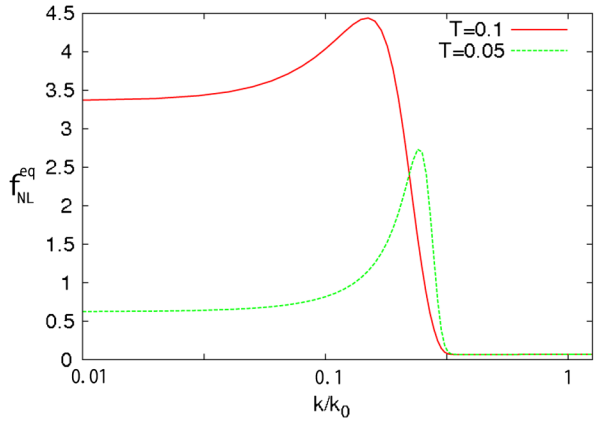

FIG. 5 (color online). We plot the equilateral bispectrum for various values of $T < 1$ with $d = 20$. They show the featured bispectra at $k/k_0 \simeq 0.1$.

When we focus on bispectrum for superhorizon scales, i.e., taking $k_1/k_0 < \mathcal{O}(1)$, all bispectra have peaks at equilateral shape affected by the effect of finite changing duration time d, otherwise the delta approximation, $d \ll 1$, also shows the local type of bispectra, which have been seen in the previous paper [24]. Our results do not depend on specifying the choice of parameter d, only when we consider a finite duration time; $d > \mathcal{O}(1)$.

Therefore, we will plot the equilateral bispectrum $f^{eq}_{NL} = f_{NL}(k_1 = k_2 = k_3)$ in Fig. 5, and Fig. 6 for various values of T with $d = 20$. We can see the featured bispectrum in Fig. 5 where we take small values of T as $T = 0.1$ and $T = 0.05$, pointing $f^{\rm eq}_{\rm NL} = \mathcal{O}(5)$ within the recent constraint. On the other hand, the cases for other values of T show no such feature in Fig. 6, where the equilateral bispectrum increases (decreases) towards super(sub)horizon scale as seen in the left (right) panel. We can also see a small feature at subhorizon scale $k/k_0 \gtrsim 1$ for the large value of $T = 10$, however this value of amplitude of the feature is too small to be detectable.

IV. CONCLUDING REMARKS

We focus on the evolution of curvature perturbation on superhorizon scales by adopting the spatial gradient expansion. We have reviewed such an approximation in both linear and nonlinear theory, which is called the *beyond* δN formalism as the next-leading order in the expansion. In our formalism [16,19], we can deal with the time evolution

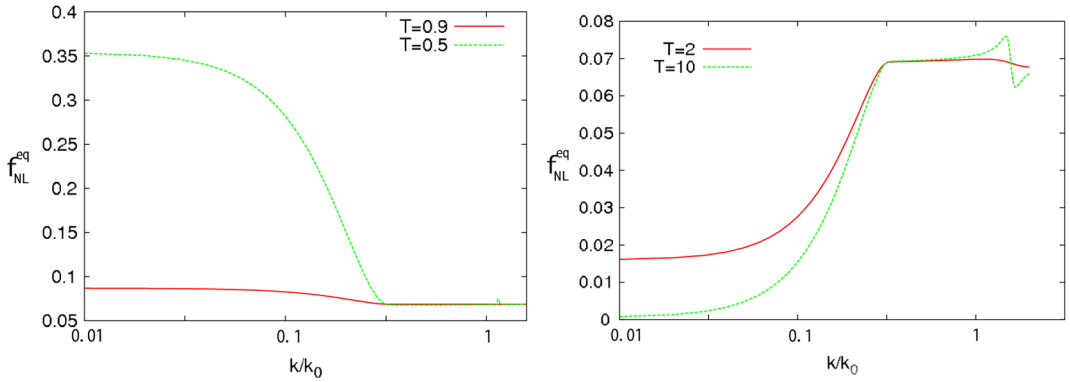

FIG. 6 (color online). The equilateral bispectrum for $T < 1$ (left) and $T > 1$ (right) with $d = 20$. Even though we can see small features at subhorizon scale $k/k_0 > 1$ for a large value of $T = 10$, the plots generally show no detectable feature.

in contrast to δN formalism, where curvature perturbations remain just constant, and nonlinear curvature perturbation follows the simple master equation whose form is similar to one in linear theory.

As seen in (2.1) and (2.5), the evolution equation for curvature perturbation in both theories takes similar structures, therefore in order to estimate the power spectrum (2.14) and bispectrum (2.21) in the approximation, all we have to do is to calculate the same integrals as D_K and F_k in the enhancement factor: α_k^{Lin} shown in (2.12). It is easy to estimate non-Gaussianity, in contrast with the usual in-in formalism [20], where a numerical calculation of the correlated function would be too difficult to solve (see also [36] for the numerical method), if one considers a complicated situation needs to be solved numerically. Beyond δN formalism takes an advantage to calculating the correlated features for power spectrum and bispectrum since the calculation is basically the same as solving the power spectrum.

As one application of our formalism for a single scalar field, we investigate the case of varying sound speed. Although the previous studies have done for the situation of a sudden changing of sound speed, in this paper we studied an effect of its changing with a finite duration time, which needs to be solved numerically. The study of [27] also investigated such mild transit in the speed of sound, but the result can be derived in the analytic way and by using a different formalism from our δN formalism. The results give the similar feature and are consistent with each other. We also notice that the study of [29] did a most recent analysis by using PLANCK data and also show such a featured bispectrum.

The main purpose of this paper is to analyze whether the features can appear in the bispectrum, in particular of equilateral shape by using our nonlinear perturbation theory. The case is more suitable to calculate by using our formalism than by using the in-in formalism. We discuss local features of primordial power and bispectrum generated by the effect of varying sound speed. As shown in [16] by using a similar way, we have also investigated one application of the beyond δN for analyzing the featured bispectrum affected by a sharp change in the inflaton's potential slope.

As shown in Fig. 5, we can see a local feature like a bump at $k/k_0 = \mathcal{O}(0.1)$ for a small value of $T = c_{s1}/c_{s2} < \mathcal{O}(0.1)$ in the equilateral bispectrum, which has a peak value of non-Gaussianity; $f_{\mathrm{NL}}^{\mathrm{eq}} = \mathcal{O}(10)$ at most, consistent within the recent observational constraint by PLANCK. However, such parameters also lead to the features in the power spectrum, which are excluded from the observations since the current CMB experiment gives a strong constraint, which is sensitive to $|T-1| \gtrsim 0.1$ by the CMB temperature power spectrum (see [23]).

This study is one toy model as a first step to investigate a more realistic situation, that is for example, including a background evolution, extending to multifield system, etc. We plan to work on this and hope to discuss them in the future.

ACKNOWLEDGMENTS

We thank Ryo Saito for useful discussion and comments. The work is supported by a Grant-in-Aid through JSPS No. 24-2236.

[1] P. Ade *et al.* (Planck Collaboration), arXiv:1303.5062.
[2] C. L. Bennett *et al.* (WMAP Collaboration), Astrophys. J. Suppl. Ser. **208**, 20 (2013).
[3] D. H. Lyth and A. Liddle, *The Primordial Density Perturbation* (Cambridge University Press, Cambridge, 2009).
[4] P. Ade *et al.* (Planck Collaboration), arXiv:1303.5082.
[5] P. Ade *et al.* (Planck Collaboration), arXiv:1303.5084.
[6] M. Sasaki and D. Wands, Classical Quantum Gravity **27**, 120301 (2010).
[7] D. S. Salopek and J. R. Bond, Phys. Rev. D **42**, 3936 (1990).
[8] Y. Nambu and A. Taruya, Classical Quantum Gravity **13**, 705 (1996).
[9] M. Sasaki and T. Tanaka, Prog. Theor. Phys. **99**, 763 (1998).
[10] D. Wands, K. A. Malik, D. H. Lyth, and A. R. Liddle, Phys. Rev. D **62**, 043527 (2000).
[11] G. I. Rigopoulos and E. P. S. Shellard, Phys. Rev. D **68**, 123518 (2003).
[12] D. H. Lyth and Y. Rodriguez, Phys. Rev. Lett. **95**, 121302 (2005).
[13] Y. Tanaka and M. Sasaki, Prog. Theor. Phys. **117**, 633 (2007).
[14] Y. Tanaka and M. Sasaki, Prog. Theor. Phys. **118**, 455 (2007).
[15] Y. Takamizu and S. Mukohyama, J. Cosmol. Astropart. Phys. 01 (2009) 013.
[16] Y. Takamizu, S. Mukohyama, M. Sasaki, and Y. Tanaka, J. Cosmol. Astropart. Phys. 06 (2010) 019.
[17] Y. Takamizu and J. Yokoyama, Phys. Rev. D **83**, 043504 (2011).
[18] A. Naruko, Y. Takamizu, and M. Sasaki, Prog. Theor. Exp. Phys. **2013**, 43E01 (2013).
[19] Y. Takamizu and T. Kobayashi, Prog. Theor. Exp. Phys. **2013**, 63E03 (2013).
[20] J. M. Maldacena, J. High Energy Phys. 05 (2003) 013.
[21] K. A. Malik and D. Wands, Classical Quantum Gravity **21**, L65 (2004).
[22] J. Khoury and F. Piazza, J. Cosmol. Astropart. Phys. 07 (2009) 026.

[23] M. Nakashima, R. Saito, Y. Takamizu, and J. Yokoyama, Prog. Theor. Phys. **125**, 1035 (2011).
[24] M. Park and L. Sorbo, Phys. Rev. D **85**, 083520 (2012).
[25] R. H. Ribeiro, J. Cosmol. Astropart. Phys. 05 (2012) 037.
[26] J. Emery, G. Tasinato, and D. Wands, J. Cosmol. Astropart. Phys. 08 (2012) 005.
[27] A. Achucarro, J. Gong, G. A. Palma, and S. P. Patil, Phys. Rev. D **87**, 121301 (2013).
[28] N. Bartolo, D. Cannone, and S. Matarrese, J. Cosmol. Astropart. Phys. 10 (2013) 038.
[29] A. Achucarro, V. Atal, P. Ortiz, and J. Torrado, arXiv:1311.2552.
[30] A. Achucarro, J. Gong, S. Hardeman, G. A. Palma, and S. P. Patil, J. Cosmol. Astropart. Phys. 01 (2011) 030.
[31] R. Saito, M. Nakashima, Y. Takamizu, and J. Yokoyama, J. Cosmol. Astropart. Phys. 11 (2012) 036.
[32] R. Saito and Y. Takamizu, J. Cosmol. Astropart. Phys. 06 (2013) 031.
[33] T. Moroi and T. Takahashi, Phys. Lett. B **522**, 215 (2001).
[34] D. H. Lyth and D. Wands, Phys. Lett. B **524**, 5 (2002).
[35] A. J. Christopherson and K. A. Malik, Phys. Lett. B **675**, 159 (2009).
[36] X. Chen, R. Easther, and E. A. Lim, J. Cosmol. Astropart. Phys. 06 (2007) 023.